Breakup of 8B and the 7Be(p,g)8B reaction

ARTICLE *in* PRAMANA · AUGUST 1999

Impact Factor: 0.65 · DOI: 10.1007/s12043-999-0036-5 · Source: arXiv

2 AUTHORS:

Radhey Shyam
Saha Institute of Nuclear Physics
151 PUBLICATIONS **1,619** CITATIONS
SEE PROFILE

Ian J Thompson
Lawrence Livermore National Laboratory
318 PUBLICATIONS **6,459** CITATIONS
SEE PROFILE

Breakup of ^{8}B and the ^{7}Be$(p,\gamma)^8$B reaction*

R. Shyam† and I.J. Thompson‡
†Saha Institute of Nuclear Physics, Calcutta, India.
‡Department of Physics, University of Surrey, Guildford, Surrey GU2 5XH, U.K.

Abstract. The calculated rate of events in some of the existing solar neutrino detectors is directly proportional to the rate of the ^{7}Be$(p,\gamma)^8$B reaction measured in the laboratory at low energies. However, the low-energy cross sections of this reaction are quite uncertain as various measurements differ from each other by 30-40 %. The Coulomb dissociation process which reverses the radiative capture by the dissociation of ^{8}B in the Coulomb field of a target, provides an alternate way of accessing this reaction. While this method has several advantages (like large breakup cross sections and flexibility in the kinematics), the difficulties arise from the possible interference by the nuclear interactions, uncertainties in the contributions of the various multipoles and the higher order effects, which should be considered carefully. We review the progress made so far in the experimental measurements and theoretical analysis of the breakup of ^{8}B and discuss the current status of the low-energy cross sections (or the astrophysical S-factor) of the ^{7}Be$(p,\gamma)^8$B reaction extracted therefrom. The future directions of the experimental and theoretical investigations are also suggested.

1. Introduction

The ^{8}B isotope produced in the Sun via the radiative capture reaction ^{7}Be(p,γ)^{8}B is the principal source of the high energy neutrinos detected in the Super-Kamiokande (SK) and ^{37}Cl detectors [1]. In fact the calculated rate of events in SK as well as SNO detectors [3] is directly proportional to the rate of this reaction measured in the laboratory at low energies ($\sim$ 20 keV) [3]. Unfortunately, the measured cross sections (at relative energies (E_{CM}) of [p $-$ ^{7}Be] $>$ 200 keV) disagree in absolute magnitude and the value extracted by extrapolating the data in the region of 20 keV differ from each other by 30-40 %. This makes the rate of the reaction ^{7}Be$(p,\gamma)^8$B the most poorly known quantity in the entire nucleosynthesis chain leading to the formation of ^{8}B [4]. It may be noted that the rate of the ^{7}Be(p,γ)^{8}B reaction is usually given in terms of the zero-energy astrophysical S-factor, $S_{17}(0)$.

The Coulomb dissociation (CD) method provides an alternative indirect way to determine the cross sections for the radiative capture reactions at low energies [5, 6, 7, 8, 9]. In this procedure it is assumed that the break-up reaction $a+Z \rightarrow (b+x)+Z$ proceeds entirely via the electromagnetic interaction; the two nuclei a and Z do not interact strongly. By further assuming that the electromagnetic excitation process is

*Work supported by EPSRC, UK, grant nos. J/95867 and L/94574

of first order, one can relate directly (see *e.g.* Refs. [5, 6]) the measured cross-sections of this reaction to those of the radiative capture reaction $b + x \rightarrow a + \gamma$. Thus, the astrophysical S-factors of the radiative capture processes can be determined from the study of break-up reactions under these conditions.

However, in the CD of ^{8}B, the contributions of $E2$ and $M1$ multipolarities can be disproportionately enhanced in certain kinematical regimes [10, 11]. Furthermore, interference from the nuclear breakup processes may also be considerable in some regions. Therefore, a careful investigation [9, 12] is necessary to isolate the conditions in which these terms have negligible effect on the calculated breakup cross sections.

Motobayshi et al. [13] have performed the first measurements (to be referred as RIKEN-I) of the dissociation of ^{8}B into the ^{7}Be$-p$ low energy continuum in the field of ^{208}Pb with a radioactive ^{8}B beam of 46.5 MeV/nucleon energy. Assuming a pure E1 excitation, the Monte Carlo simulation of their data predicts a $S_{17}(0) = 16.7 \pm 3.2$ eV barn, which is considerably lower than the value of 22.4 $\pm$2.0 eV barn used by Bahcall and Pinsonneault [2] in their standard solar model (SSM) calculations. This generated a lot of interest in the studies of the breakup reactions of ^{8}B. Since, under the kinematical conditions of the RIKEN-I experiment the $E2$ component of breakup may be disproportionately enhanced, attempts were made to determine this component by extending the angular range of the measurements in the RIKEN-I data in a repeat experiment [14] (to be referred as RIKEN-II) to larger angles which are expected to be more sensitive to this multipolarity. On the other hand, measurements of the breakup of ^{8}B were also carried out at subCoulomb beam energies [15] where $E2$ multipolarity is expected to dominate according to the semiclassical theory of the Coulomb excitation [16]. Measurements of the breakup of ^{8}B have also been performed at the relativistic energies of 250 MeV/nucleon at GSI Darmstadt.

In this review, we present the latest status of the analysis of the available experimental data on the breakup of ^{8}B and of the extracted S_{17} value therefrom. Results obtained from the both semiclassical and full quantum mechanical calculations are discussed in the next two sections. Conclusions and the outlook in presented in section 4.

2. Semiclassical calculations

2.1. RIKEN data, $E_{beam} \sim$ 50 MeV/nucleon

An analysis of the RIKEN-I data was presented in [7], where the breakup cross sections of ^{8}B corresponding to $E1$, $E2$ and $M1$ multipolarities were calculated within a semiclassical theory of Coulomb excitation, which included simultaneously the effects of Coulomb recoil and relativistic retardation. This was achieved by solving the general classical problem of the motion of two relativistic charged

particles [17]. The role of the nuclear excitations was also investigated by performing full quantum mechanical calculation of the Coulomb, nuclear as well as of their interference terms, using a collective model prescription for the nuclear form factor. It was found that nuclear effects modify the pure Coulomb amplitudes very marginally in the entire kinematical regime of the RIKEN-I data.

The double differential cross-section for the Coulomb excitation of a projectile from its ground state to the continuum, with a definite multipolarity of order $\pi\lambda$ is given by [5, 6, 7]

$$\frac{d^2\sigma}{d\Omega dE_\gamma} = \sum_{\pi\lambda} \frac{1}{E_\gamma} \frac{dn_{\pi\lambda}}{d\Omega} \sigma_\gamma^{\pi\lambda}(E_\gamma), \quad (1)$$

where $\sigma_\gamma^{\pi\lambda}(E_\gamma)$ is the cross-section for the photodisintegration process $\gamma + a \rightarrow b + x$, with photon energy E_γ, and multipolarity π = E (electric) or M (magnetic), and $\lambda = 1, 2...$ (order), which is related to that of the radiative capture process $\sigma(b + x \rightarrow a + \gamma)$ through the theorem of detailed balance. In terms of the astrophysical S-factor, $S(E_{cm})$, we can write

$$\sigma(b + x \rightarrow a + \gamma) = \frac{S(E_{cm})}{E_{cm}} \exp(-2\pi\eta(E_{cm})), \quad (2)$$

where $\eta = \frac{Z_b Z_x e^2}{\hbar v}$, with v, Z_b and Z_x being the relative center of mass velocity, and charges of the fragments b and x respectively.

In most cases, only one or two multipolarities dominate the radiative capture as well as the Coulomb dissociation cross sections. In Eq. (1) $n_{\pi\lambda}(E_\gamma)$ represents the number of equivalent (virtual) photons provided by the Coulomb field of the target to the projectile, which is calculated by the method discussed in Ref. [7, 17] . $S(E_{cm})$, can be directly determined from the measured Coulomb dissociation cross-sections using Eqs. 1 and 2.

In Fig. 1, we show the comparison of the calculated [7] Coulomb dissociation double differential cross sections with the corresponding data of Ref. [13] as a function of the scattering angle θ_{cm} of the excited ^{8}B (center of mass of the ^{7}Be+p system) for three values of the E_{cm}. The calculated $E1$, $E2$ and $M1$ cross sections are folded with an efficiency matrix provided to us by the RIKEN group. The solid lines in Fig. 1 show the calculated $E1$ cross sections obtained with S-factors (S_{17}) that provide best fit to the data (determined by χ^2 minimization procedure). These are (17.58 ± 2.26) eV barn, (14.07 ± 2.67) eV barn and (15.59 ± 3.49) eV barn at E_{cm}= 0.6 MeV, 0.8 MeV and 1.0 MeV respectively. By using a direct extrapolation procedure, the best fit "$E1$ only" S_{17} factors, give a $S_{17}(0) = (15.5 \pm 2.80)$ eV barn.

The contributions of the $E2$ and $M1$ excitations are calculated by using the radiative capture cross sections $\sigma(p+^7\text{Be} \rightarrow ^8\text{B}+\gamma)$, given by the models of Typel and Baur (TB) [18] and Kim, Park and Kim (KPK) [19]. We have used as input the corresponding S factors averaged over energy bins of experimental uncertainty in the relative energy of the fragments. In Fig. 1, the dashed (dashed dotted) line

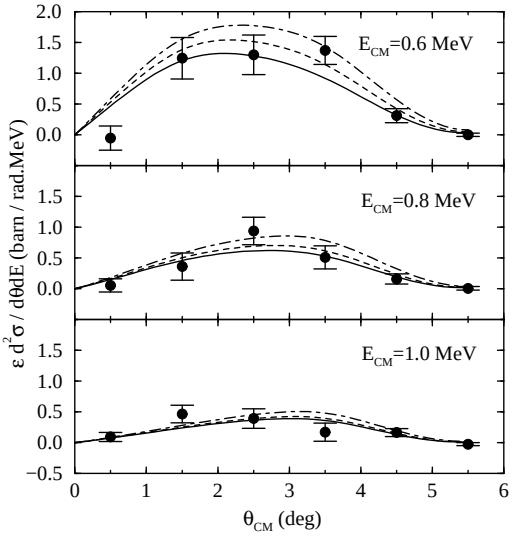

Figure 1: Comparison of experimental and theoretical Coulomb dissociation yields (cross section × detector efficiency) as a function of θ_{cm} for the E_{cm} values of 0.6 MeV, 0.8 MeV and 1.0 MeV. Solid lines show the calculated pure $E1$ Coulomb dissociation cross sections obtained with best fit values of S factors as discussed in the text. The dashed and dashed dotted curves represent the sum of $E1$, $E2$ and $M1$ contributions with latter two components calculated with capture cross sections given in the models of TB [18] and KPK [19] respectively. The experimental data is taken from Ref. [13].

shows the $E1$ (with best fit S_{17}) + $E2$ + $M1$ cross sections, with $E2$ and $M1$ components calculated with TB (KPK) capture cross sections. It is clear that the magnitude of the $E2$ contributions to the RIKEN-I data depend significantly on the nuclear structure model used to calculate the corresponding capture cross sections, and it is difficult to draw any definite conclusion about the extent of its role in the RIKEN-I data from this analysis. The $M1$ component contributes insignificantly and unlike the $E2$ component it not as model dependent.

Since at larger scattering angles, the angular distributions of the Coulomb breakup of ^{8}B are expected to be more sensitive to the $E2$ component, the RIKEN group has repeated their experiment [14] where the angular range of the data was extended up to 9°. In Fig. 2, we show a comparison of the calculated Coulomb dissociation cross sections for the double differential cross sections with the RIKEN-II data. In these calculations the capture cross sections have been taken from Esbensen and Bertsch [20], which predicts a $S_{17}(0) = 18.5$ ev barn. Since we have not used any arbitrary normalization constant in the theoretical calculations shown in this figure, RIKEN-II data seems to be consistent with a slightly larger value of $S_{17}(0)$ as compared to RIKEN-I. We also note that while the $E2$ component contributes

significantly to the total cross sections at all the angles in the energy bin 2000-2250 keV, it is dominant beyond 6° in the lower energy range of E_{CM}. However, at larger angles the nuclear breakup effects are also expected to be more important. Therefore, it would be necessary to include these effects before drawing any conclusion about the role of $E2$ multipolarity in this data.

In Ref. [14], an analysis of the data was performed within the distorted wave Born-approximation including the nuclear effects, where it was concluded that the $E2$ component and the nuclear breakup effects are considerably smaller. However, they use a collective model prescription to calculate the inelastic nuclear form factor (see eg. [7]). Due to a long tail in the ^{8}B g.s wave function this procedure is unlikely to be accurate. Furthermore, Coulomb breakup is calculated by a point-like projectile approximation (PLPA) in these studies (and also in the semiclassical calculations presented above), and its range of validity is yet to be determined for this projectile.

It is therefore, necessary to perform a full quantal mechanical analysis of the RIKEN-II data in order to check the validity of various assumptions of the Coulomb dissociation method. This will be presented in section 3.

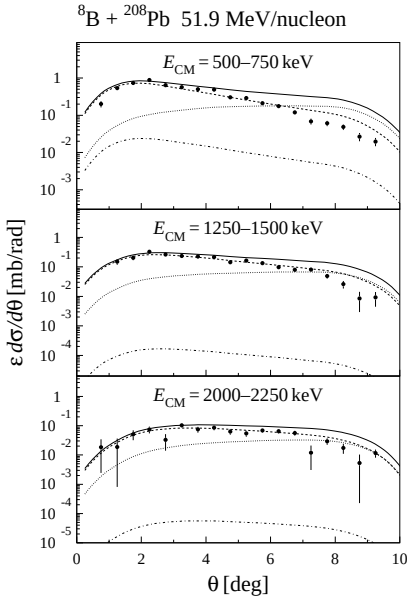

Figure 2: $E1$ (dashed line), $E2$ (dotted line), and $M1$ (dashed-dotted line) components of the Coulomb dissociation cross section $\epsilon d\sigma/d\theta$ as a function of the scattering angle in the dissociation of ^{8}B on ^{208}Pb target at the beam energy of 51.9 MeV/nucleon. The solid line shows their sum. Results for relative energy bins of (a) 500-750 keV, (b) 1250-1500 keV and (c) 2000-2250 keV are shown. ϵ is the detector efficiency. The experimental data and ϵ are taken from Ref. [14].

2.2. Notre Dame data, E_{beam} = 25.8 MeV

The Notre Dame group has measured the breakup of ^{8}B on the ^{58}Ni target at the beam energy of 25.8 MeV, well below the Coulomb barrier, where the $E2$ component is expected to dominate the CD process [15]. However, the reliable extraction of the $E2$ component from this data, where only the the integrated cross section of the ^{7}Be fragment is measured, is still doubtful. The analysis of the data reported in Ref. [15] used the Alder-Winter's semiclassical theory of Coulomb excitation, where the final state is treated as a two-body system, thus assuming that the measured angles of ^{7}Be were equal to those of the ^{7}Be-p center of mass. The inadequacy of this assumption has been demonstrated in [8]. Furthermore, the total breakup cross section reported in this experiment could not be reproduced within the Alder-Winther theory even if a wide variety of structure models of ^{8}B were used [21]. Therefore, the uncertainty about the magnitude of the $E2$ cross section calculated with various structure models of ^{8}B is not eliminated by the Notre Dame measurements [15].

Furthermore, the importance of the nuclear breakup effects in the kinematical regime of the Notre Dame experiment has been emphasized in Ref. [22]. Therefore, there is a need to reanalyze this data using a quantum mechanical theory where the nuclear excitations and the three-body kinematics are taken into account.

3. Full Quantum Mechanical calculations

A one-step prior-form DWBA analysis of the ^{8}B breakup data has been reported in [9] at both low and high energies in order to check the validity of various assumptions of the Coulomb dissociation method. The breakup process is described as a single proton excitation of the projectile from its ground state to a range of states in the continuum, which is discretized by the method of continuum bins. Excitations to states corresponding to the relative energy (of the $p - ^7 Be$ system) up to 3.0 MeV and relative partial waves up to 3 have been taken into account. The point-like projectile approximation as well as collective model prescription for the nuclear form factor have been avoided, by determining the nuclear and Coulomb parts by a single-folding method where the relevant fragment-target interactions are folded by the projectile wave functions in the ground and continuum states.

3.1. ^8B Breakup at $\sim$ 50 MeV, RIKEN data

In Fig. 3a, $E1$ and $E2$ components of the angular distributions for the ^{8}B + ^{208}Pb $\rightarrow$ ^{8}B* + ^{208}Pb reaction measured by the Kikuchi et al. [14] at the beam energy of 415 MeV are shown, for the pure Coulomb excitation case. The dashed, dotted and solid lines represent $E1$, $E2$ and $E1 + E2$ cross sections respectively which are obtained by the single-folding procedure. Also shown in this figure are the corresponding results obtained by PLPA (curves with solid circles). We note that

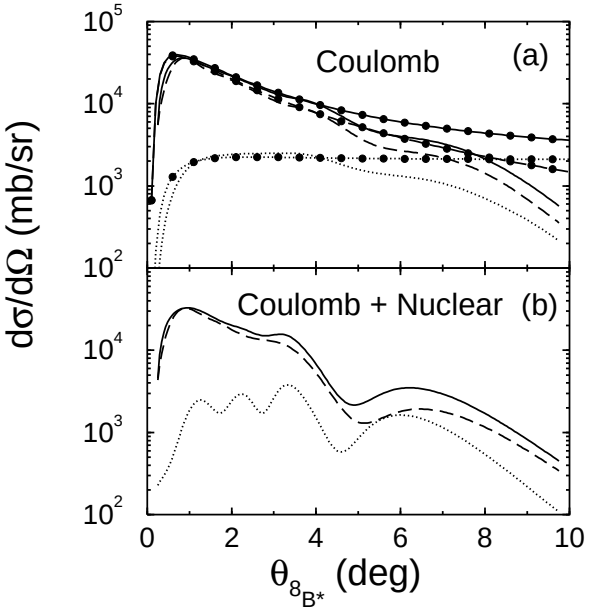

Figure 3: Angular distribution for ^{8}B+^{208}Pb → ^{8}B*(^{7}Be+p)+ ^{208}Pb reaction at the beam energy of 415 MeV. (a) Results for pure Coulomb excitation, the dashed and dotted curves represent the $E1$ and $E2$ cross sections while their sum is depicted by the solid line. Also shown here are the results obtained with a point-like projectile approximation (Alder-Winther theory), where dashed and dotted lines with solid circles show the corresponding $E1$ and $E2$ cross sections while the solid line with solid circles represents their sum. (b) Coherent sum of Coulomb and Nuclear excitation calculations; the dashed and dotted lines show the dipole and quadrupole components while the solid line is their sum.

PLPA becomes inaccurate beyond 4° in this case. Moreover, the $E2$ component of the pure Coulomb excitation becomes increasingly important also after this angle.

In Fig. 3b, the cross sections obtained by summing coherently the Coulomb and nuclear amplitudes (to be referred as *total* in the following) are shown. The dashed and dotted lines show the dipole and quadrupole cross sections respectively, while the solid line represents their sum. It can be noted that nuclear effects modify the pure Coulomb $E1$ cross sections substantially after $\sim 4°$, and the $E2$ cross sections in the entire angular range. However, since the $E2$ components are quite small at angles $\leq 4°$, the difference between pure Coulomb and *total* dipole + quadrupole cross sections is appreciable only after this angle.

Therefore, at RIKEN energies, the PLPA breaks down beyond 4°, where the Coulomb-nuclear interference effects as well as the quadrupole component of breakup is substantial. Hence, the Coulomb dissociation method as used in e.g.

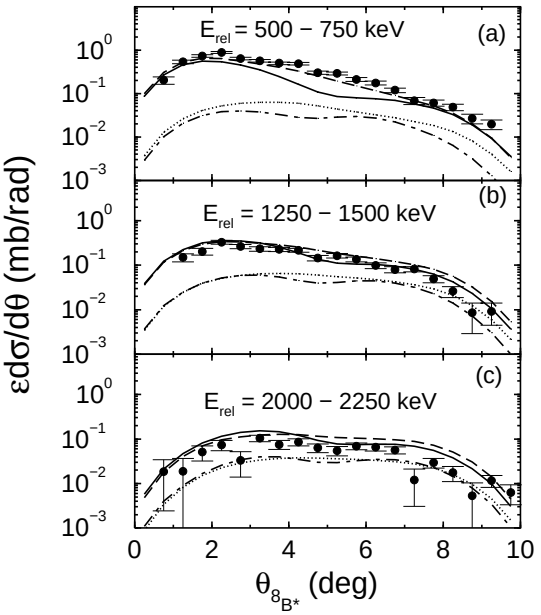

Figure 4: Comparison of experimental and theoretical cross section $\epsilon d\sigma/d\theta$ as a function of the scattering angle $\theta_{^8B^*}$ for ^{8}B+^{208}Pb $\rightarrow$ ^{8}B*(^{7}Be+p)+ ^{208}Pb reaction at the beam energy of 415 MeV. Results for three relative energy bins of (a) 500-750 keV, (b) 1250-1500 keV, (c) 2000-2250 keV are shown. ϵ is the detector efficiency. Solid lines show the calculated total Coulomb plus nuclear dissociation cross sections while the dashed lines represents the corresponding pure Coulomb dissociation result. Pure quadrupole Coulomb and Coulomb+nuclear cross sections are shown by dotted and dashed-dotted lines. The experimental data and the detector efficiencies are taken from [14].

Ref. [7] to extract $S_{17}(0)$ from the measurements of the angular distributions in the breakup of ^{8}B on heavy target at RIKEN energies ($\sim$ 50 MeV/nucleon), is reliable only when data is taken at angles below 4°.

In Figs. 4a, 4b and 4c the comparison of calculations [9] for $\epsilon \cdot d\sigma/d\theta$ with the experimental data of Kikuchi et al. [14] is shown as a function of the scattering angle $\theta_{^8B^*}$ of the excited ^{8}B (center of mass of the ^{7}Be+p system) for three relative energy bins. The efficiency (ϵ) matrix as well as angular and energy averaging were the same as those discussed in Ref. [14]. The dashed and dotted lines are the pure Coulomb $E1$+$E2$ and $E2$ cross sections respectively while the solid and dashed lines are the corresponding *total* cross sections. We note that the calculations are in fair agreement with the experimental data. No arbitrary normalization constant has been used in the results reported in this figure.

The quadrupole component of breakup is significant at almost all the angles in

the relative energy bin 2.0 – 2.25 MeV(c), and at angles beyond 5° in the energy bin 1.25 – 1.50 MeV(b). On the other hand, its contribution is inconsequential in the energy bin 0.5 – 0.75 MeV (a). This result is in somewhat disagreement with that reported in Ref. [14], where this component is reported to be small everywhere below 1.75 MeV relative energy. Although these authors also perform a quantum mechanical calculation within DWBA, their treatment of the continuum state is very different from that of Ref. [9]. Moreover they use a collective model prescription for the Coulomb and nuclear form factors, which has a limited applicability for ^{8}B breakup. Bertulani and Gai [12] have also reported smaller quadrupole component in their analysis of this data. These authors do not include the nuclear effects in the $E1$ excitations and make use of the eikonal approximation to calculate the quadrupole nuclear excitation amplitudes. Moreover, the Coulomb excitation amplitudes have been calculated with the PLPA which have been found to be invalid at higher angles (see Fig. 3). It is also noted in Fig.3 that Coulomb-nuclear interference effects reduce the $E1$ cross sections at larger angles.

Some authors have studied the importance of the higher order effects in the Coulomb breakup of ^{8}B [24, 20, 26]. At RIKEN energies these effects play only a minor role for this reaction in the kinematical regime of forward angles and low relative energies [24, 20, 26]. Therefore, the conclusions arrived in Ref. [9] about the RIKEN data are unlikely to be affected much by the higher order breakup effects. However, the multi-step breakup could play an important role at Notre Dame energies, which is discussed in [23].

3.2. ^8B breakup at subCoulomb energies, Notre Dame data

In Figs. 5a and 5b, the calculated angular distributions [9] of ^{7}Be and ^{8}B* respectively in a ^{8}B induced breakup reaction on ^{58}Ni target are shown, at the beam energy of 25.8 MeV. Pure Coulomb and pure nuclear breakup cross sections are represented by the dashed and dashed-dotted curves respectively. The *total* cross sections are represented by the solid lines. In these calculations also the procedure of single-folding the respective fragment-target interactions with ^{8}B ground and continuum state wave functions have been used. One can see that the angular distributions of ^{7}Be and ^{8}B* are distinctly different from each other. While pure Coulomb and *total* breakup cross sections show a forward peak in case of ^{7}Be (which is typical of the angular distribution of fragments emitted in breakup reactions), those of ^{8}B* tend to zero as angle goes to zero. The latter is the manifestation of the adiabatic cut-off typical of the Coulomb-excitation process. In both the cases the nuclear effects are small below 20° and there is a Coulomb-nuclear interference minimum between 25° - 60°. However the magnitude of various cross sections are smaller in Fig. 5a. Furthermore, the nuclear-dominated peak occurs at different angles in Figs 5a ($\simeq 55°$) and 5b ($\simeq 70°$). As discussed in [8], the angles of ^{7}Be can be related to those of ^{8}B*. A given $\theta_{^7Be}$ gets contributions from a range of generally larger $\theta_{^8B^*}$. This could explain the shifting of the peaks of various curves to lower angles in Fig. 5a as compared to the corresponding ones in Fig. 5b. This underlines the important of three-body kinematics in describing the inclusive breakup reactions.

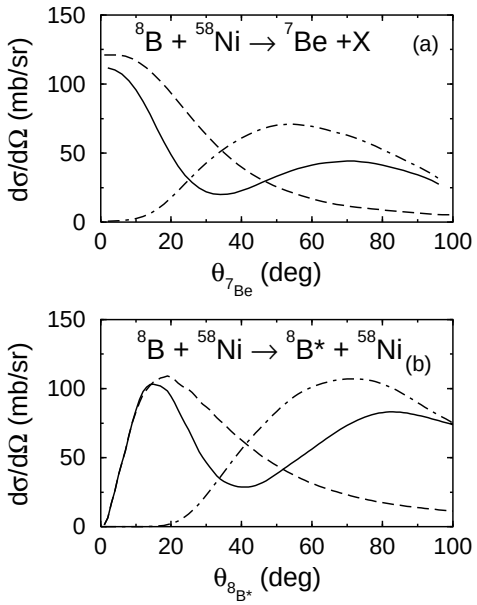

Figure 5: (a) Angular distribution of the ^{7}Be fragment emitted in the breakup reaction of ^{8}B on ^{58}Ni target at the beam energy of 25.8 MeV. The dashed and dashed-dotted lines show the pure Coulomb and pure nuclear breakup cross sections respectively while their coherent some is represented by the solid line. (b) Angular distribution of ^{8}B* in the Coulomb excitation of ^{8}B on ^{58}Ni at the beam energy of 25.8 MeV. The dashed and dashed-dotted lines show the cross sections for pure Coulomb and pure nuclear excitation respectively, while the solid line represents their coherent sum.

The ratio of the experimental integrated breakup cross section of ^{7}Be (obtained by integrating the breakup yields in the angular range, $(45 \pm 6)^\circ$, of the experimental setup) to Rutherford elastic scattering of ^{8}B is reported to be $(8.1 \pm 0.8^{+2.0}_{-0.5}) \times 10^{-3}$ [15]. It is not possible to get this cross section by directly integrating the angular distributions shown in Fig. 4b in this angular range as the corresponding angles belong to ^{8}B* and not to ^{7}Be. However, in the three-body case (Fig. 5a), this can be done in a straight-forward way. This gives a value of 7.0×10^{-3} which is in close agreement with the experimental data. Thus, previous failures to explain the experimental value may be attributed to the neglect of both the Coulomb-nuclear interference effects and the three-body kinematics.

In Fig. 6, the range of the validity of the point-like projectile approximation (PLPA) and the role of the Coulomb-nuclear interference effects on the cross sections of dipole and quadrupole components is investigated. In Fig. 6a the results for pure Coulomb breakup are shown. Dipole and quadrupole components of the cross section obtained by the single-folding procedure are shown by solid and dashed lines

respectively, while those obtained with the PLPA by solid and dashed lines with solid circles. It can be noted that PLPA is not valid for angles beyond 20°. The condition that the impact parameter of the collision is larger than the sum of the projectile and target radii ($b > R_a + R_t$), assumed in applying the Alder-Winther theory, is no longer valid because there is a long tail in the ^{8}B ground state wave function. We also note that the quadrupole component is affected more by the PLPA as compared to the dipole. The big difference in the dipole and quadrupole cross sections seen in the PLPA results beyond 20° (where the quadrupole component is much bigger than the dipole), almost disappears in the corresponding cross sections obtained by single-folding procedure. Nevertheless, the quadrupole cross sections still remain larger than those of the dipole beyond 30° in the latter case.

In connection with PLPA, it should be made clear that p + target and the ^{7}Be + target potentials *do* take into account the finite size of the ^{7}Be and target nuclei. This effect, however, is only important when two nuclei are very close to each other and is masked by the nuclear effects which would be important at those impact parameters.

Dipole and quadrupole cross sections for pure nuclear breakup are shown in Fig. 6b. The cross sections obtained by summing coherently the amplitudes of $E1$ and $E2$ components of pure Coulomb and pure nuclear breakup are shown in Fig. 6c. We notice that the Coulomb-nuclear interference effects make the contributions of the dipole component of the *total* cross section larger than those of quadrupole one at all the angles. This result is quite remarkable as it implies that the $E2$ component of the total break up cross section in the ^{8}B induced reaction on ^{58}Ni target is not dominant even at the subCoulomb beam energies. Therefore, there is hardly any hope of determining the $E2$ component of ^{8}B breakup by Notre Dame type of experiment [15].

This underlines the need for more refined experiments to determine the $E2$ component. It is clear from Fig. 6c that the measurements of the angular distributions may provide useful information about the $E2$ component as it is different from that of the $E1$ multipolarity. On the other hand, the angular distributions of the fragments, calculated within a semiclassical theory without making the approximation of isotropic angular distributions in the projectile rest frame, have been shown to have large $E1$ - $E2$ interference effects [20]. They lead to asymmetries in the momentum distributions of the fragments, whose measurements may enable one to put constraints on the $E2$ component [27]. However, for the better accuracy of this method, improved calculations including the nuclear effects may be necessary.

These results for the nuclear effects in the angular distribution of ^{8}B* are approximately similar to those reported in [28], where Coulomb and nuclear form factors are calculated by folding the proton-target mean-field (parameterized by a Woods-Saxon function) by the ground and discretized continuum state ^{8}B wave functions. These authors calculate various cross sections by integrating a fixed projectile-target optical potential along a semiclassical trajectory. However, since the three-body kinematics for the final state has not been considered by them, a direct comparison between their calculations and the data of [15] is not possible.

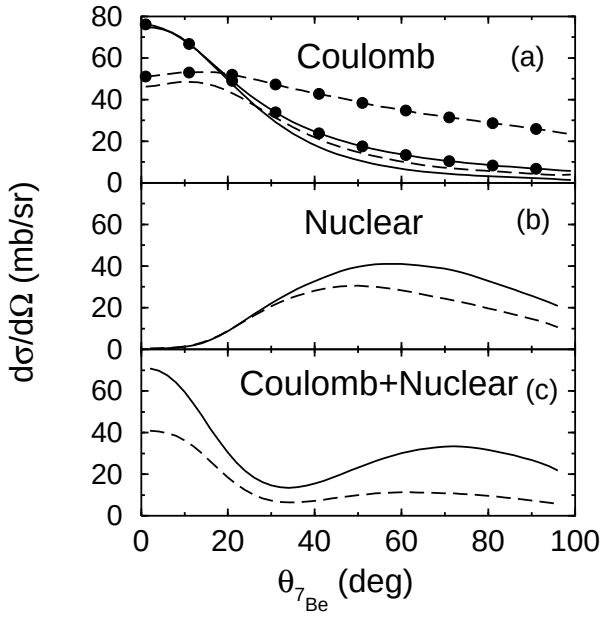

Figure 6: Dipole (solid lines) and quadrupole (dashed lines) components of the angular distributions of the ^{7}Be fragment emitted in the breakup reaction of ^{8}B on ^{58}Ni target at the beam energy of 25.8 MeV. (a) pure Coulomb breakup; also shown here are the $E1$ (solid lines with solid circles) and $E2$ (dashed lines with solid circles) cross sections obtained with point-like projectile and target approximation (Alder-Winther theory), (b) pure nuclear breakup and (c) Coulomb plus nuclear breakup where the corresponding amplitudes are coherently summed.

4. Summary and Conclusions

The Coulomb dissociation method provides a useful tool to calculate the cross sections of the difficult-to-measure time-reversed processes (ie. radiative capture reactions) of astrophysical interest. Application of this method in determining the low-energy cross sections of the $^{7}\mathrm{Be}(p,\gamma)^{8}\mathrm{B}$, which is of considerable interest in the context of the Solar Neutrino problem, has yielded some interesting results since the first pioneering experiment performed at RIKEN on the $^{8}\mathrm{B} + {}^{208}\mathrm{Pb} \rightarrow {}^{8}\mathrm{B}^{*} + {}^{208}\mathrm{Pb}$ at beam energies around 50 MeV/nucleon. Detailed theoretical analysis (within the one-step distorted wave Born approximation) reveal that RIKEN-I and RIKEN-II data are almost free from the nuclear effects and are dominated by the $E1$ component for ^{7}Be-p relative energies < 0.75 MeV at very forward angles ($\leq 4^{\circ}$). The study of the breakup of ^{8}B in this kinematical regime is, therefore, better suited for the extraction of a reliable $S_{17}(0)$ for the capture reaction $^{7}\mathrm{Be}(p,\gamma)^{8}\mathrm{B}$ at low relative energies.

For the breakup reaction at low energy the Coulomb-nuclear interference effects

are quite important. A very striking feature of this effect is that it makes the $E1$ component of the *total* cross section of the breakup reaction ^{8}B + ^{58}Ni → ^{7}Be + X (at the beam energy of 25.8 MeV), larger than the corresponding $E2$ component at all the angles. This renders untenable the main objective of the Notre Dame experiment of determining the $E2$ component in the breakup of ^{8}B at low beam energies. The dominance of the $E2$ component for this reaction at this energy, seen in the semi-classical Alder-Winther theory of Coulomb excitation has led to this expectation. However, we note that even in pure Coulomb dissociation process, with finite size of the projectile taken into account, the $E2$ components is almost equal to that of $E1$ in the relevant angular range.

It can be said that the feasibility of the Coulomb dissociation method in determining the $S_{17}(0)$ from the breakup reactions of ^{8}B has been established by identifying the kinematical regime where the assumptions of this method are well fulfilled. We now have all the theoretical tools to analyze such experiments, and a reliable value of S_{17} by means of the Coulomb dissociation method may be extracted soon.

References

[1] J.N. Bahcall, Neutrino Astrophysics, Cambridge University Press, New York (1989)
[2] J.N. Bahcall, M.H. Pinsonneault, Rev. Mod. Phys. **69** (1995) 781.
[3] J.N. Bahcall, Nucl. Phys. **A 631** (1998) 29.
[4] E.G. Adelberger et al., Rev. Mod. Phys. **70** (1998) 1265.
[5] G. Baur and H. Rebel, J. Phys.G : Nucl. and Part. Phys. **20** (1994) 1.
[6] G. Baur and H. Rebel, Ann. Rev. Nuc. Part. Sc. **46** (1997) 321.
[7] R. Shyam, I.J. Thompson and A.K. Dutt-Majumder, Phys. Lett. **B 371** (1996) 1.
[8] R. Shyam and I.J. Thompson, Phys. Lett. **B 415** (1997) 315.
[9] R. Shyam and I.J. Thompson, Phys. Rev. **C 59** (1999) 2465.
[10] K. Langanke and T.D. Shoppa, Phys. Rev. C **49** (1994) R1771; **51** (1995) 2844(E); **52** (1995) 1709.
[11] M. Gai and C.A. Bertulani, Phys. Rev. C **52** (1995) 1706.
[12] C.A. Bertulani and M. Gai, Nucl. Phys. A **636** (1998) 227.
[13] T. Motobayashi et al., Phys. Rev. Lett. **73** (1994) 2680.
[14] T. Kikuchi et al., Phys. Lett. **B 391** (1997) 261.
[15] Johanes von Schwarzenberg *et al.*, Phys. Rev. C **53** (1996) R2598.
[16] K. Alder and A. Winther, *Electromagnetic Excitation* (North-Holland, Amsterdam, 1975).
[17] A.N.F. Alexio and C.A. Bertulani, Nucl. Phys. **A 505** (1989) 448.
[18] S. Typel and G. Baur, Phys. Rev. C **50** (1994) 2104
[19] K.H. Kim, M.H. Park, and B.T. Kim, Phys. Rev.C **35** (1987) 363.
[20] H. Esbensen and G.F. Bertsch, Nucl. Phys.A **600** (1996) 37.
[21] F.M. Nunes, R.Shyam and I.J. Thompson, J. Phys.G: Nucl & Part Phys. **24** (1998) 1575.
[22] F.M. Nunes and I.J. Thompson, Phys. Rev. **C 57** (1998) R2818.
[23] F.M. Nunes and I.J. Thompson, Phys. Rev. **C 59** (1999) 2652.
[24] S. Typel and G. Baur, Phys. Rev.C **50**, 2104 (1994).
[25] H. Esbensen, G.F. Bertsch and C.A. Bertulani, Nucl. Phys. A **581**, 107 (1995).
[26] S. Typel, H. Wolter and G. Baur, Nucl. Phys.A **617**, 147 (1997).
[27] B. Davids et al., Phys. Rev. Lett. **81**, 2209 (1998).
[28] C.H. Dasso, S.M. Lenzi and A. Vitturi, Nucl. Phys. A. **639** (1999) 635.